2

Large-Scale Synthesis of Semiconductor Nanowires by Thermal Plasma

Peng Hu, Fangli Yuan and Yajun Tian
State Key Laboratory of Multi-phase Complex Systems,
Institute of Process Engineering,
Chinese Academy of Sciences, Beijing,
China

1. Introduction

One-dimensional (1D) semiconductor nanostructures, classified as nanowires, nanobelts and nanotubes, have shown superior properties in electric, chemical, mechanical and optical fields (Li et al., 2004; Pan et al., 2001; Pavesi et al., 2000; Q. Wang et al., 2008), and can be served as the fundamental building blocks for constructing advanced inter-connectors and nanoscale electronic, optoelectronic and sensing nanodevices (Duan et al., 2001; Huang et al., 2001; Lao et al., 2003; X.D. Wang et al., 2007). In general, the design of 1D nanostructure emphasizes to strength the growth of crystal along one direction and restrict other two dimensions to nanosize. In recent years, considerable achievements have been made on preparation of 1D nanostructures and different synthetic strategies have been developed to fabricate various 1D nanostructures, including element (Nikoobakht & El-Sayed, 2003; Lu et al., 2005; Vivekchand et al., 2004; Wirtz & Martin, 2003), oxide (Dai et al., 2003; Ohgi et al., 2005; Wu et al., 2005; Zheng et al., 2002), nitride (Kim et al., 2002; Toury et al., 2003), sulfide (Gao et al., 2005; Kar & Chaudhuri, 2005; Zhu et al., 2003), and others (Hornbostel et al., 1995; Jun et al., 2006; X.Y. Wang et al., 2002), which makes it possible to further investigate their properties and applications in nanodevices. In this chapter, we will review the recent development achieved primarily from the author's studies addressing the key issues of semiconductor 1D nanostructures by thermal plasma, including the growth, characterization and applications of obtained products based on their unique properties related to this special synthetic route.

2. General background of thermal plasma

Plasma typically refers to the fourth state of matter similar to gas in which a certain portion of the species is ionized, containing ions, electrons, atoms and neutral species (Boulos, 1991, 2004). Based on the thermodynamic equilibrium between the gas species, plasmas can be classified as equilibrium, local equilibrium and non-equilibrium plasma. In equilibrium plasma, the gas species are nearly fully ionized with same temperature and the plasma temperature is extremely high, as we called astrophysical plasmas (such as sun). In local equilibrium plasma, only a small fraction of the gas molecules are ionized while the electrons and heavy particles approximately have the same temperature and show local

electrical neutrality, in which the plasma temperature is still typically several thousand degrees and generally is called thermal plasma. While in non-equilibrium plasma, the electron temperature is still typical several thousand degrees but the temperature of heavy neutrals is rather low, and the plasma exhibits ambient temperature so we call them cold plasma.

Thermal plasmas can be generated at atmospheric pressure or under soft vacuum conditions for a wide range of gases, providing an inert, oxidizing or reducing atmosphere for the needs of materials processing. Typical examples of thermal plasmas include various forms of direct current (DC) arcs and radio frequency induction (RF) plasma discharges. Compare with other technology routes, the typical features of thermal plasma are high temperature up to 2000～20000K and charged particle density in the range of 10^{19}～10^{21} per m^3. The high temperature, enthalpies and heat fluxes in the plasma torch make it suitable to apply in many chemical synthesis and metallurgical processes, and the presence of active ions species in plasma can also promote the chemical activity of reaction species. The flexibility of starting materials with solid, liquid, gas or in combination and react environment with inert or reactive gas in the plasma reactor make it versatile in producing a variety of materials including metals, carbides, nitrides, oxides or composites of materials with well dispersed and definite size. It's fast quenching rate at flame tail can 'freeze' the particles in an intermediate state and gives the materials with novel structures and properties.

3. Growth of 1D semiconductor nanostructures by RF thermal plasma

The RF thermal plasma generally includes a refractory and a quartz tube in which working gas flows, and the plasma is generated through electromagnetic coupling of the RF power supply through the induction coil surrounding the tube by partially ionizing the working gas within the tube. The plasma gas does not come in contact with electrodes and eliminates possible sources of contamination and allows for operation with a wide range of gases, including inert, reducing, oxidizing and other corrosive atmospheres. Accordingly, the plasma so generated is called inductively coupled plasma or induction plasma, and Figure 1 shows the experimental plasma torch by argon discharge.

Fig. 1. Photograph of induction plasma generated by argon discharge

In plasma synthesis process, the starting materials are feed into the plasma by carrier gas and subsequently heated to melt ever vaporize. The axial feeding way and long particle residence time within the discharge zone provide the enough heat transfer from the plasma to the particles. During the following process, reaction and growth processes are occurred in flowing gas in the reactor, and the final products are collected at the bottom of the collector. The schematic illustration of plasma system is shown in Figure 2 (Hu et al., 2007).

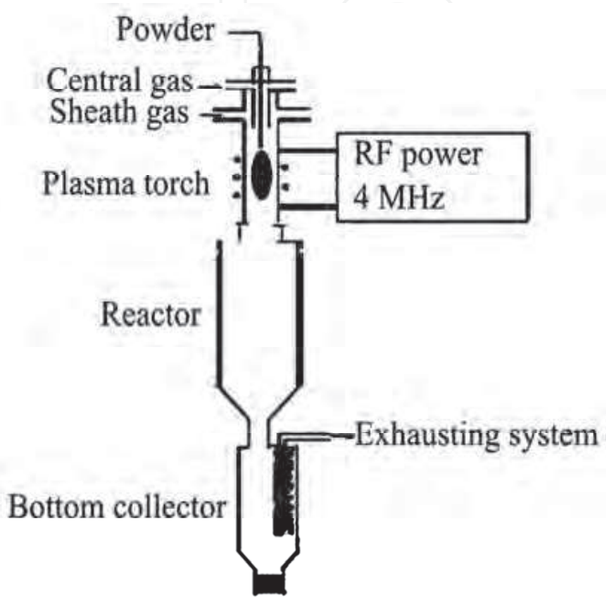

Fig. 2. Schematic illustration of the plasma system (Hu et al., 2007)

3.1 ZnO nanowires

3.1.1 Synthesis and structure control

For ZnO nanowires synthesis, zinc was used as starting materials and supplied into the plasma flame by carrying gas with a feed rate of 20～50 g/min and then underwent vaporization, oxidation, crystallization and growth processes following the flowing gas, finally obtained products. Argon (1.0 m^3/h) and nitrogen gas (5.0 m^3/h) were injected as the plasma-forming gas and sheath gas, respectively. The chamber pressure was maintained at atmospheric pressure. Specially, oxygen gas was injected into the system together with the sheath gas to oxidize the zinc powder.

After the experiment, white woollike ZnO products were obtained in the collector, and the morphology and structural investigation of synthesized products are shown in Figure 3. Figure 3a gives the typical SEM image of obtained products, which reveals the formation of large scaled ZnO with uniform morphology in the products. Magnified SEM image shown in Figure 3b indicates that as-synthesized products are composed of rodlike nanostructures with uniform diameter of about 50 nm along the stem. All the peaks in the XRD pattern of the sample can be well indexed to the hexagonal ZnO wurtzite structure as shown in Figure 3c. From the TEM images shown in Figure 3d and e, we can see that the nanowires with typical length about 2 μm and diameter about 50 nm are obtained, and the tips of two ends exhibit round shape. HRTEM image in Figure 3f reveals the perfect monocrystalline structure of obtained products.

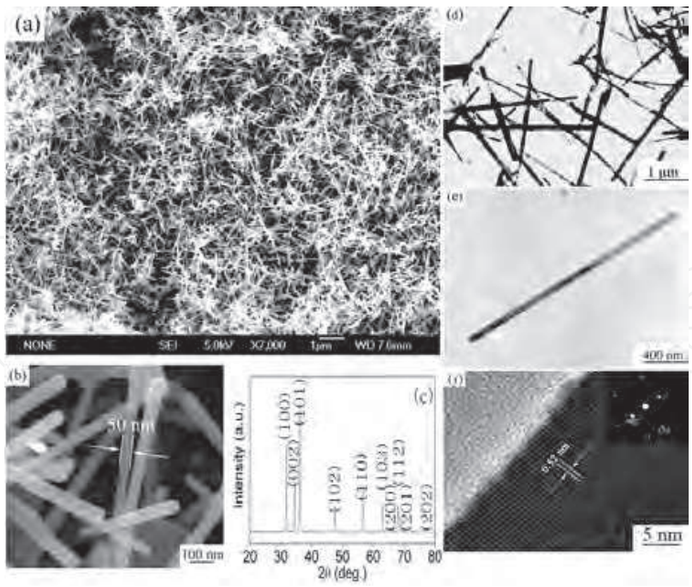

Fig. 3. (a) SEM image, (b) Magnified SEM image, displaying the uniform diameter, (c) XRD pattern, (d) low-magnification TEM image, (e) TEM image of single crystal and (f) HRTEM image of synthesized ZnO products (Hu et al., 2007)

In plasma synthesis process, starting materials, oxygen partial pressure and supersaturation of zinc vapor in the plasma play key roles in the growth of the nanowires. By controlling the species and feedstock rate of the starting material, and the flow rate of oxygen gas, the 1D structure with different morphology could be well adjusted, such as nanowires with different ratio of length to diameter, tetrapods and multipods.

3.1.2 Growth rate of nanowires in plasma

In our synthesis process, the resident time of particles in reactor is very short and as a result the growth rate of products should be very fast to grow into rodlike nanostructure with length of several micrometers. According to the reactor length and diameter, and the gas flow rate in it, the resident time can be calculated as 0.15 seconds under the typical experimental conditions. In another word, the axial growth rate is about 13 μm/s for the nanowire with length about 2 μm, which is rather fast than the time needed for nanowire synthesized by the predominant vapor deposition process and wet chemist routes.

The high growth rate of nanowire in plasma synthesis process can be explained by the crystal growth dynamics theory similar to that occurred in solvent, in which supercooling degree promotes the nucleation and growth of the crystal, and high level degree of undercooling provides intensive growth driver for reactive species to nucleate and grow into crystal. However, too much degree of undercooling decreases the diffusion of nucleating substances in solvent, and lead to the formation of crystal with small size. In plasma synthesis process, vapor species with several thousands degrees are first formed due to the high processing temperature in the flame zone and then cooled to form ultrahigh-level supercooling vapor in the plasma tail, which provides intensive growth driver for ZnO to nucleate and grow. In addition, part of zinc and oxygen was ionized in the plasma zone, which accelerates the transmittability of electrons from zinc to oxygen. All of these provide intensive growth driver for ZnO to nucleate and growth with high growth rate. However,

the nanowires with small length are achieved when too much degree of undercooling was realized by introducing excess cooling gas to the reactor, and the results are well in accordance with the crystallization process in solvent.

3.1.3 Growth mechanism of nanowires in plasma

In our experiment, no substrate or catalysts are used to confine the growth direction of nanorods, and the basic phenomena involved in the crystal growth are an in-flight way. That is to say, all the growth processes of nanowires are occurred exclusively in flow gas. Since there is no involvement of catalysts or templates to serve as energetic favorable sites for the absorption of reactant molecules or to confine the growth direction of nanowires, it would be reasonable to imagine that the morphology of obtained products is determinate by the growth habit of crystals. ZnO belongs to hexagonal phase crystal which has the anisotropic growth nature. When ZnO crystal grows, anisotropic growth habit prefers the crystal to grow along the C axis and forms columnar structure. As a result, the crystal structure of the products may be the underlying factor that determines the formation of 1D nanostructure in plasma.

The growth process of nanowire via gas phase reaction typically involves the vapor-liquid-solid (VLS) process and vapor-solid (VS) process (Wagner & Ellis, 2004; Yang & Lieber, 1996; Zhang et al., 2001). In our experiment, no metal catalysts were used and the typically round tips in the end of the synthesized nanorods confirm that growth mechanism of nanorods is governed by the VS mechanism, but this process is exactly not the same as the references reported previously, in which the nanorod grows along one direction. In our products, the round tips on the two ends of the nanorods suggested that the nanorods were grown in two directions along the [0001] axis. The schematic of the growth mechanism is shown in Figure 4a. To investigate the growth mechanism more clearly, a contrasting experiment was carried out with increased temperature gradient. Figure 4b shows the TEM image of as-synthesized products, and a double-directional needlelike nanostructures were obtained, which reveals that the nanorods are governed by a wall-free and two direction growth mechanism.

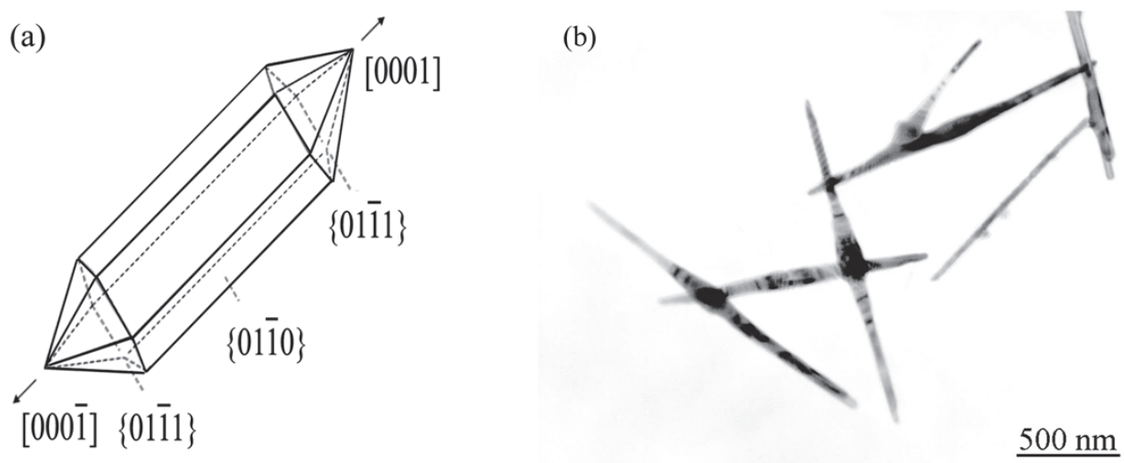

Fig. 4. (a) the schematic of the growth mechanism and (b) TEM image of synthesized double-direction needlelike nanostructures (Hu et al., 2007)

3.1.4 Properties and applications

3.1.4.1 Photocatalytic activities under visible light

Some interesting properties are found for our synthesized nanowires and Figure 5a gives the photocatalytic activities of synthesized ZnO nanocrystals under visible light irradiation. From the patterns we can see that as-synthesized products exhibit excellent photodegradation effect for methyl red solution and photocatalytic activity can be significantly improved by increasing the length of nanowires. After visible light irradiation for 12 h, the concentration for nanowires with length of 2 μm is about 45%, which is about 2-fold lower than that of nanowires with length of 200 nm. Figure 5b demonstrates the color change of methyl red solution using 2 μm nanowires as photodegradation agent and a translucence solution can be observed after 20 h visible light irradiation, which indicates the obvious photocatalytic effect of obtained ZnO nanowires.

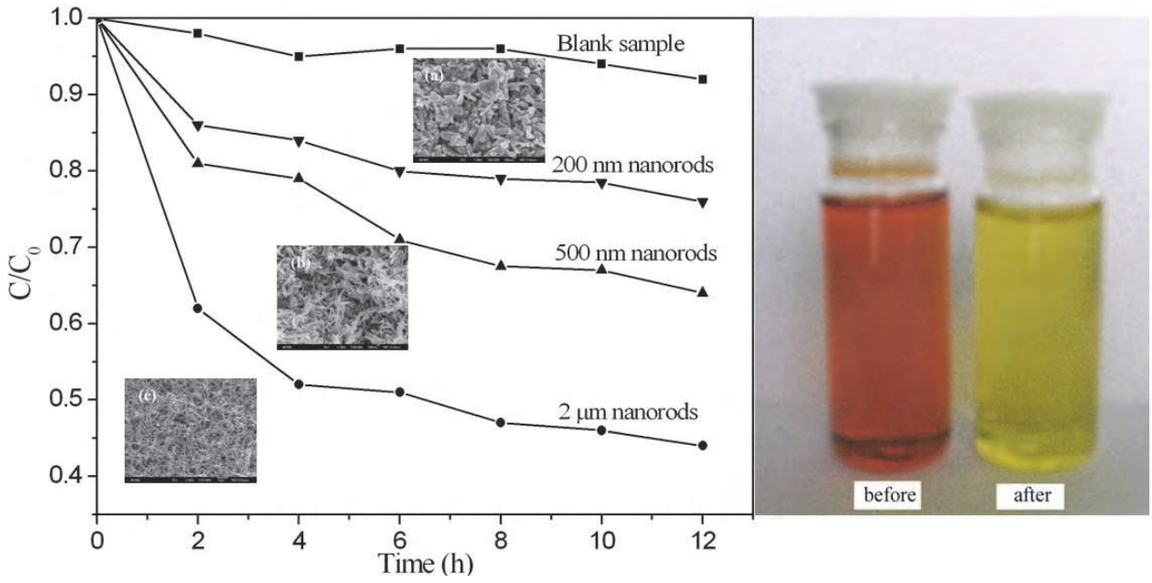

Fig. 5. (a)Photocatalytic activities of synthesized ZnO nanocrystals under visible light irradiation and (b) photodegradation effect of methyl red solution under 20 h visible light irradiation

It is known that ZnO is an n-typed semiconductor with band-gap energy of 3.2 eV and thus only absorbs UV light with the wavelength less than 385 nm. However, as far as photocatalytic efficiency and practical applications are concerned, it is desirable that ZnO absorbs not only UV but also visible light because visible light accounts for about 45% energy of solar radiation. Because of the semiconducting property of ZnO crystal, the visible-light absorption could be obtained by n-typed doping (such as transitional metal ions) but hard to achieved by p-typed doping (such as N). In our experiment, implanting nitrogen into ZnO crystals was achieved by introducing nitrogen gas into the plasma sheath gas and carrier gas, and visible light absorbing was obtained by narrowing or splitting the band gap of ZnO into several sub-gaps. The doping content of nitrogen element is measured to be several hundreds ppm by chemical composition analysis of obtained nanowires.

3.1.4.2 Nanowire based gas sensor

The gas sensing property of obtained nonowires (shown in Figure 6) was tested using formaldehyde gas as working gas in a home-made instrument as we reported earlier (Han et al., 2009), which demonstrates the high gas sensing property of plasma synthesized ZnO nanowires comparing to the literature (Bie et al., 2007; Patil et al., 2007). From the patterns

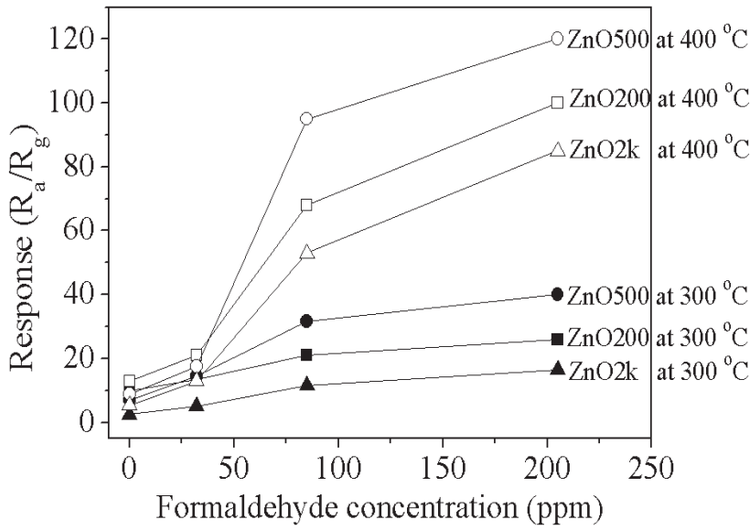

Fig. 6. Formaldehyde responses of the ZnO nanorods (tested at 300 ◦C and 400 ◦C at RH 70%) (Han et al., 2010)

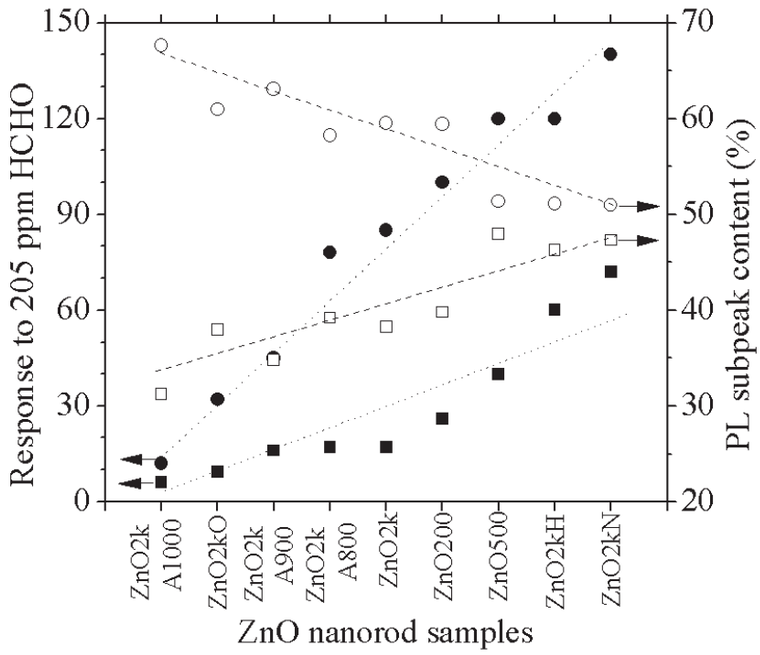

Fig. 7. Relationship between formaldehyde response of the ZnO nanowires at 300 ◦C (■) & 400 ◦C (●) and the DL (□) & AL (○) subpeaks contents (Han et al., 2010)

we can see that ZnO with length about 500 nm performed the highest gas response at both 300 ^{o}C and 400 ^{o}C, followed by ZnO nanowires with length about 200 nm and 2 μm, respectively. The difference in their gas response of obtained nanowires could be explained by the intrinsic defects in obtained products and the highest gas response of the nanowires with length about 500 nm could be contribute to the high donor-related and low acceptor-related crystal defects. Further, this conclusion is verified by annealing the ZnO nanowires in different atmosphere to adjust different defect density and related gas sensing property shown in Figure 7.

3.2 ZnS 1D nanostructures

ZnS is an important II–VI group semiconductor compound with hexagonal crystal structure that exhibits excellent properties in optical and optoelectronic fields, and its 1D nanostructures can also be obtained in plasma synthesis process. In a typical synthesis process, the staring materials of Zn and S powder (-200 mesh) were firstly mixed together (according to the mole ratio of 1:1) and then fed into the plasma by carrier gas (nitrogen gas, at a flow rate of 150 L/h) in a continuous way at different experimental parameters, such as feed rate and cooling gas rate. Figure 8 represents the ZnS 1D nanostructures synthesized at

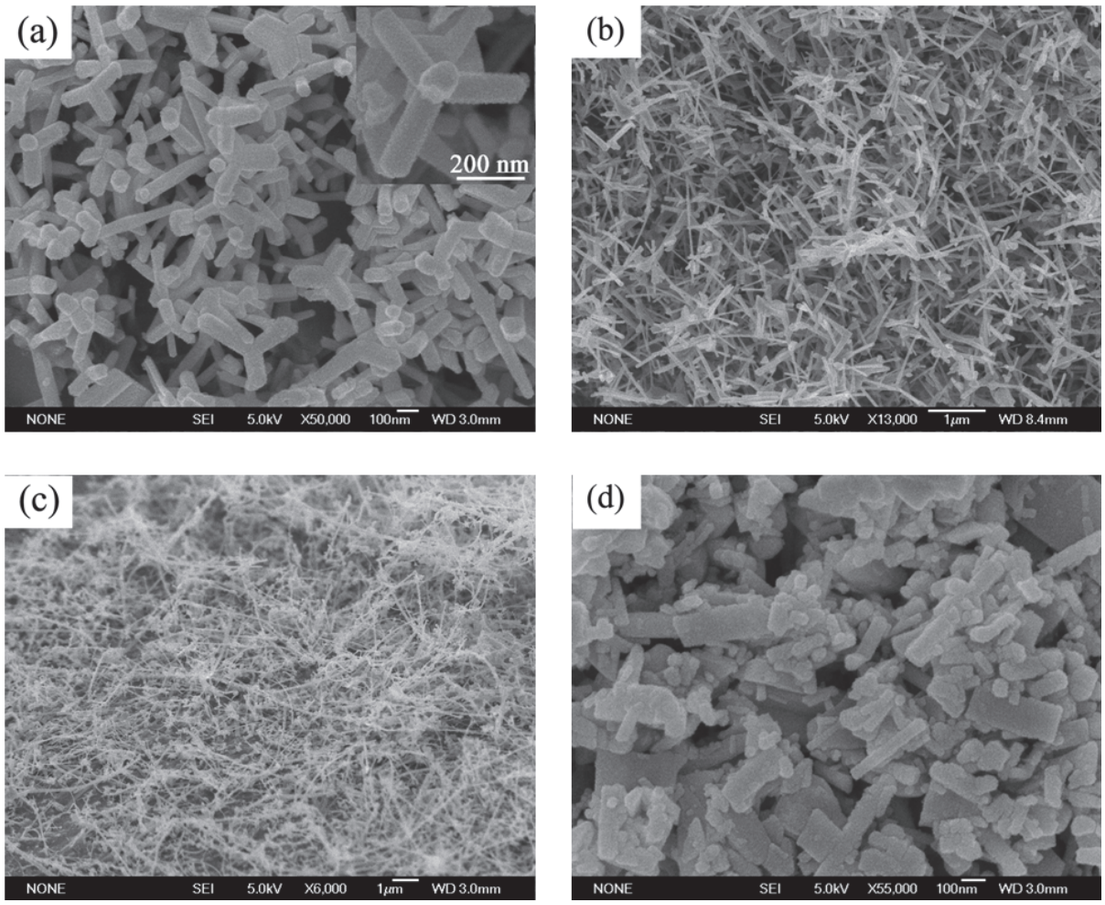

Fig. 8. SEM images of ZnS nanostructures produced with different sets of feeding rate and cooling gas flow rate (a) 12 g/min and without cooling gas, (b) 24 g/min and without cooling gas, (c) 21 g/min and with cooling gas 3 m^3/h and (d) 21 g/min and with cooling gas 6 m^3/h (Hu et al., 2009)

different conditions, and from the images we can conclude that different 1D nanostructures, including tetrapods, nanorods, nanobelts and nanoslices could be selectively synthesized by controlling the experimental parameters. Further investigation on their structures by TEM and HRTEM reveals that the 1D nanostructures are all single crystalline and hexagonal elongation along the c-axis according to the theoretical and crystal habit of the ZnS.

One of the important features of plasma synthesis route is its rather rapid growth rate compared with the conventional vapor deposition process. Meanwhile, rapid growth rate also causes the formation of intrinsic defects in crystal and Figure 9 demonstrates the existence of two different crystal defects in synthesized products. Figure 9a illustrates the stacking fault existed in a single nanobelt, which is parallel to the axis and runs through out the nanobelt. Figure 9b shows two types of structure zone existed in a leg of tetrapod ZnS. One consists of the wurtzite structure (hcp, hexagonal close-packed) in zone a and the other is sphalerite structure (fcc, face centered cubic) in zone b, and the two different structures were formed by changing the stacking sequence of the closed-packed planes of the ZnS crystal and resulted from the crystallogenesis of ZnS. It should be noted that some properties, such as the photoluminescence, gas sensing property of obtained products are closely related to the intrinsic defects in crystals (Jiang et al., 2003).

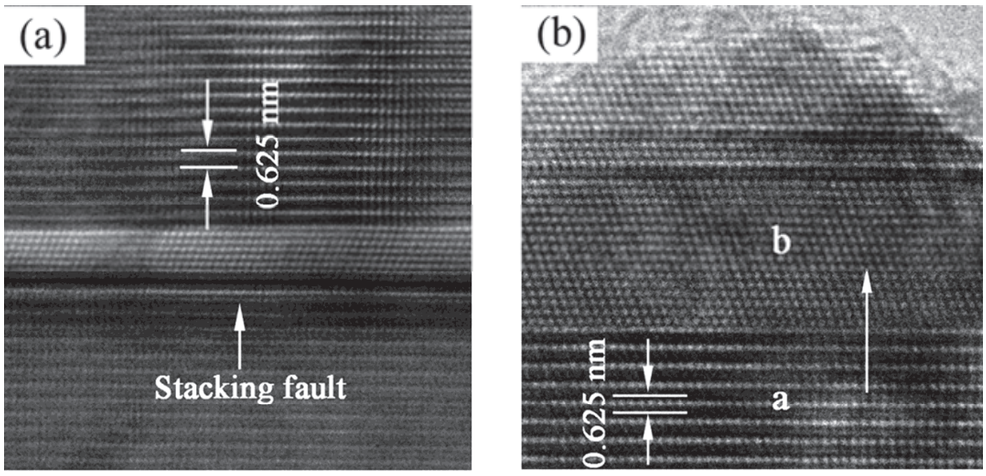

Fig. 9. The crystal defects exist in the ZnS nanocrystals (a) stacking fault in a nanobelt and (b) the sphalerite structure and the wurtzite structure polytypes in a leg of tetrapod (Hu et al., 2009)

It is worth noting that hollowing effect of 1D nanostructures was observed from products collected inner the reactor wall closed to plasma torch and the TEM images are shown in Figure 10. Structure analysis confirms that the hollow structure is resulted from the oxidation process of the ZnS nanocrystals. In our experiment, low concentration of oxygen gas was introduced into the plasma due to the impurity of the nitrogen gas and argon gas, and the oxygen gas was then heated to an ultra-high temperature and partially atomized even ionized in the plasma flame due to the effect of plasma electromagnetic field, which makes oxygen with high activity. The oxidation reaction was occurred on the surface of the crystals when the atomized oxygen contacts with the products attached on the reactor wall, and the core evacuation was underwent with the diffusion of S from inner core to outward. The hollow structures were final formed when the core was consumed completely, which is kind of similar to the formation of hollow structures by Ostwald ripening process observed in solution synthesis (Ball & Ruben 2004; Hu et al., 2008; Liu & Zeng, 2005; Zott, 2003).

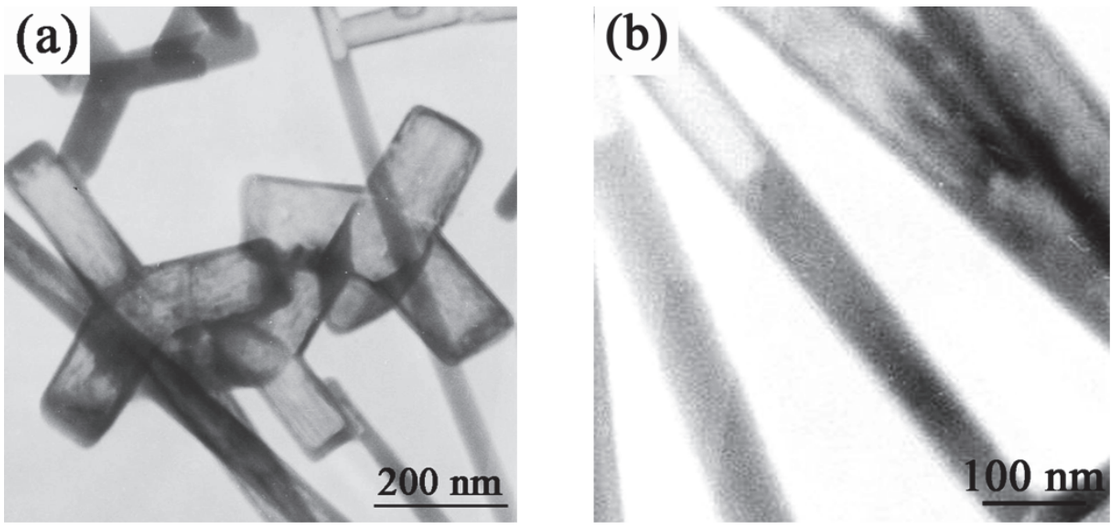

Fig. 10. TEM images of hollowing process in (a) tetrapod and (b) nanowire (Hu et al., 2009)

3.3 Transition metal doped 1D nanostructures

In addition, transition metal doped 1D nanostructures could also be obtained by adding the transition metal corresponding halides to starting materials. The synthesis process is same to that for pure binary compounds and Figure 11 demonstrates an example of the Ni doped ZnS 1D nanostructures, which reveals the versatility of plasma route for 1D nanostructures synthesis. The hysteresis loop of obtaind 1D structures shows a clear ferromagnetic behavior caused by Ni doping (shown in Figure 12) and can be adjusted by controlling the morphology of as-synthesized products.

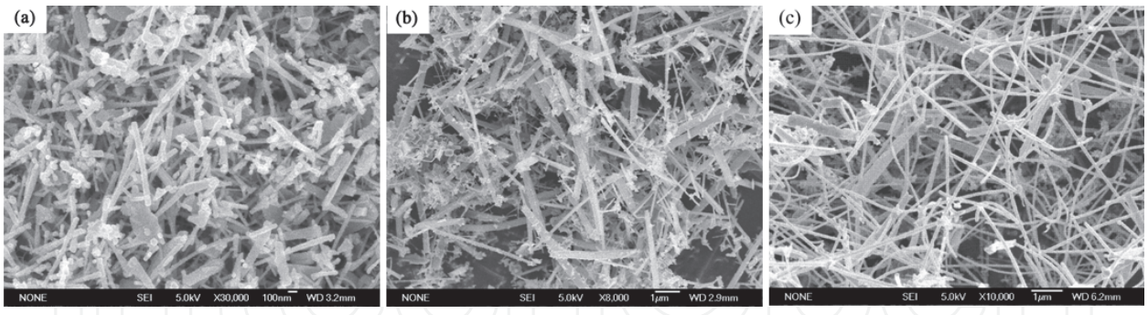

Fig. 11. SEM images of Ni doped ZnS 1D nanostructures: (a)nanorods, (b)nanobelts and (c) nanowires

3.4 Other 1D nanostructures synthesized by RF plasma

Since the morphology of products in plasma synthesis is governed by the growth habit of materials, it is reasonably believed that other materials with hexagonal crystal structure could grow into 1D nanostructures by plasma process and here we give some examples to prove this view. Figure 13 represents some examples of the 1D materials with hexagonal crystal structure grown by plasma synthesis route, and the results well confirm the growth mechanism we proposed previously. Accordingly, the plasma synthesis method provides a facile and large scale way to synthesize 1D nanostructures by a wall-free growth process.

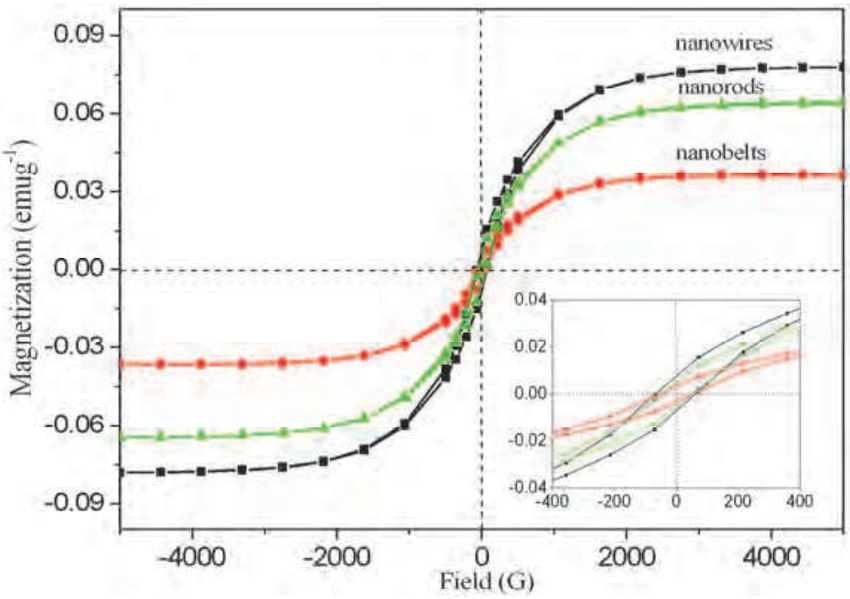

Fig. 12. Hystersis loops of Ni doped ZnS nanostructures with different morphology (a) nanowires (b) nanobelts and (c) nanorods

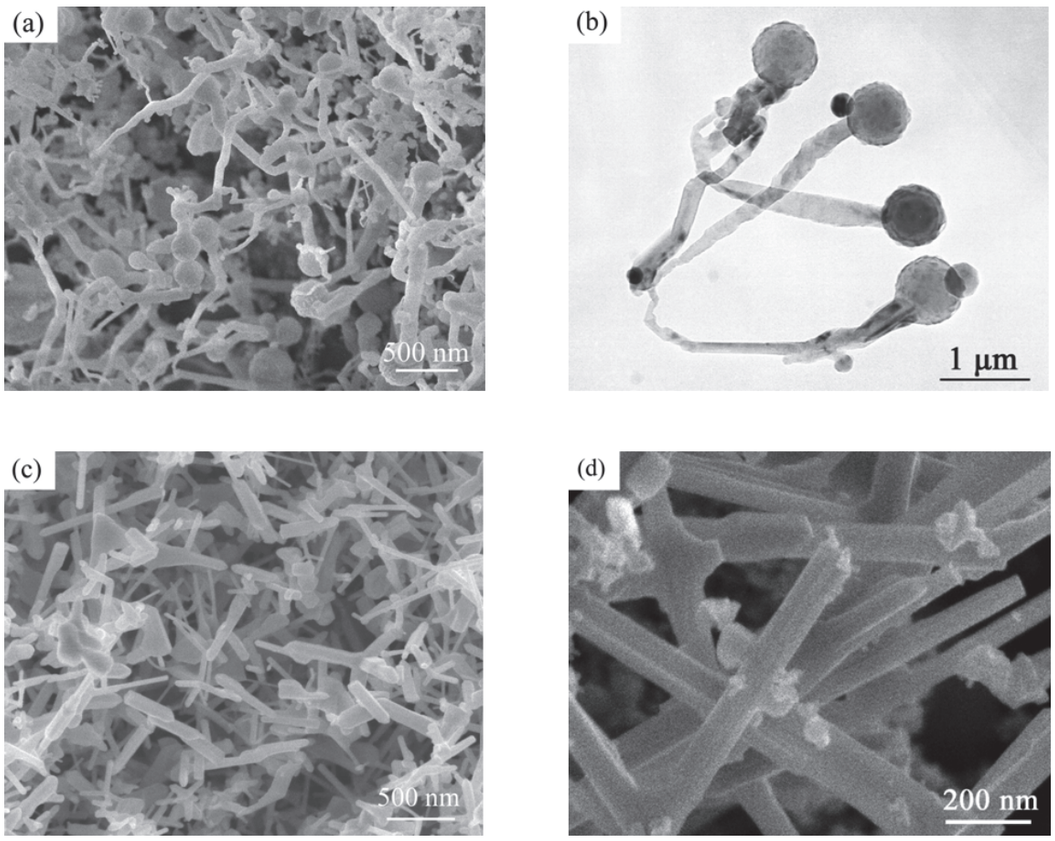

Fig. 13. Different 1D nanostructures synthesized by RF plasma (a) SEM and (b) TEM of AlN, SEM of (c) Zn and (d) WO_3

4. Conclusions

Semiconductor nanowires possess attractive electronic and photonic properties for potential applications in various nanodevices. In order to realize their device applications in real life, several problems must be solved, including controlled synthesis of semiconductor nanowires with commercial cost and achievement of nanodevices with high efficiency. This needs to develop the facile synthetic strategies and well understand the properties of obtained semiconductor nanowires. In this chapter, an overview of the recent progress in research on the large scale synthesis of semiconductor nanowires by plasma was presented, and the growth mechanism, fundamental properties and their applications are also involved. In general, the plasma synthesis process involves the vaporization, reaction, crystallization and growth processes of reactive species by an in-flight way with yield of about 10-50 g/min., which also gives the products some novel properties comparing to other synthetic strategies. With the promising approaches reviewed in the chapter and more have be achieved and to be developed, practical applications of semiconductor nanowires are imminent.

5. Acknowledgements

This work was supported financially by the National Natural Science Foundation of China (NSFC 50974111, 10905068, 20976182)

6. References

Ball, P. & Ruben, M. (2004). Color Theory in Science and Art: Ostwald and the Bauhaus. *Angewandte Chemie International Edition*, Vol.43, No.37, (September 2004), pp.4842-4847, ISSN 0570-0833

Bie, L. J.; Yan, X. N.; Yin, J.; Duan, Y. Q. & Yuan, Z. H. (2007). Nanopillar ZnO Gas Sensor for Hydrogen and Ethanol. *Sensors and Actuators B: Chemical*, Vol.126, No.2, (October 2007), pp.604-608, ISSN 0925-4005

Boulos, M. (1991). Thermal Plasma Processing. *IEEE Transactions on Plasma Science*, Vol.19, No.6, (December 1991), pp.1078-1089, ISSN 0093-3813

Boulos, M. (2004). Plasma Power Can Make Better Powders. *Metal Powder Report*, Vol.59, No.5, (May 2004), pp.16-21, ISSN 0026-0657

Dai. Z. R.; Pan. Z. W. & Wang. Z. L. (2003). Novel Nanostructures of Functional Oxides Synthesized by Thermal Evaporation. *Advanced Functional Materials*, Vol.13, No.1, (January 2003), pp.9-24, ISSN 1616-301X

Duan, X. F.; Huang, Y.; Cui, Y.; Wang, J. F & Lieber, C. M. (2001). Indium Phosphide Nanowires as Building Blocks for Nanoscale Electronic and Optoelectronic Devices. *Nature*, Vol.409, No.6816, (January 2001), pp. 66-69, ISSN 0028-0836

Gao, P.; Xie, Y.; Ye, L. N.; Chen, Y. & Guo, Q. X. (2006). From 2D Nanoflats to 2D Nanowire Networks: A Novel Hyposulfite Self-Decomposition Route to Semiconductor FeS_2 Nanowebs. *Crystal Growth & Design.* Vol.6, No.2, (Februry 2005), pp.583-587, ISSN 1528-7483

Han, N.; Tian, Y. J.; Wu, X. F. & Chen, Y. F. (2009). Improving Humidity Selectivity in Formaldehyde Gas Sensing by a Two-Sensor Array Made of Ga-Doped ZnO. *Sensors and Actuators B: Chemical*, Vol.138, No.1, (April 2009), pp.228-235, ISSN 0925-4005

Han, N.; Hu, P.; Zuo, A. H.; Zhang, D. W.; Tian, Y. J. & Chen, Y. F. (2010). Photoluminescence Investigation on the Gas Sensing Property of ZnO Nanorods Prepared by Plasma-Enhanced CVD Method. *Sensors and Actuators B: Chemical*, Vol.145, No.1, (March 2010), pp.114-119, ISSN 0925-4005

Hornbostel, M. D.; Hillyard, S.; Silcox, J. & DiSalvo, F. (1995). Nanometer width molybdenum selenide fibers. *Nanotechnology,* Vol.6, No.3, (July 1995), pp87-92, ISSN 0957-4484

Hu, P.; Yuan, F. L.; Bai, L. Y.; Li, J. L. & Chen, Y. F. (2006). Plasma Synthesis of Large Quantities of Zinc Oxide Nanorods. *The Journal of Physical Chemistry C*, Vol.111, No.1, (January 2007), pp.194-200, ISSN 19327447

Hu, P.; Yu, L. J.; Zuo, A. H.; Guo, C. Y. & Yuan, F. L. (2008). Fabrication of Monodisperse Magnetite Hollow Spheres. *The Journal of Physical Chemistry C*, Vol.113, No.3, (January 2009), pp.900-906, ISSN 1542-3050

Hu, P.; Bai, L. Y.; Yu, L. J.; Li, J. L.; Yuan, F. L. & Chen, Y. F. (2009). Shape-Controlled Synthesis of ZnS Nanostructures: A Simple and Rapid Method for One-Dimensional Materials by Plasma. *Nanoscale Research Letters*, Vol.4, No.9, (June 2009), pp.1047-1053, ISSN 1556-276X

Huang, M. H.; Mao, S.; feick, H.; Yan, H. Q.; Wu, Y. Y.; Kind, H.; Weber, E.; Russo, R. & Yang, P. D. (2001). Room-Temperature Ultraviolet Nanowire Nanolasers. *Science*, Vol.292, No.5523, (June 2001), pp.1897-1899, ISSN 0036-8075

Jiang, Y.; Meng, X. M.; Liu, J.; Xie, Z. Y.; Lee, C. S. & Lee, S. T. (2003). Hydrogen-Assisted Thermal Evaporation Synthesis of ZnS Nanoribbons on a Large Scale. *Advanced Materials*, Vol.15, No.4, (February 2003), pp.323-327, ISSN 1521-4095

Liu, B. & Zeng, H. C. (2005). Symmetric and Asymmetric Ostwald Ripening in the Fabrication of Homogeneous Core-Shell Semiconductor. *Small*, Vol.1, No.5, (May 2005), pp.566-571, ISSN 1613-6829

Jun, Y. W.; Choi, J. S. & Cheon, J. (2006). Shape Control of Semiconductor and Metal Oxide Nanocrystals through Nonhydrolytic Colloidal Routes. *Angewandte Chemie International Edition*, Vol.45, No.21, (May 2006), pp.3414-3439, ISSN 0570-0833

Kar, S. & Chaudhuri, S. (2005). Controlled Synthesis and Photoluminescence Properties of ZnS Nanowires and Nanoribbons. *The Journal of Physical Chemistry B*, Vol.109, No.8, (March 2005), pp.3298-3302, ISSN 0022-3654

Kim, H. M.; Kim, D. S.; Kim, D. Y.; Kang, T. W.; Cho, Y. H. & Chung. K. S. (2002). Growth and characterization of single-crystal GaN nanorods by hydride vapor phase epitaxy. *Applied physics Letters*, Vol.81, No.12, (September 2002), pp. 2193-2195, ISSN 0003-6951

Lao, J. Y.; Huang, J. Y.; Wang, D. Z. & Ren, Z. F. (2002). ZnO Nanobridges and Nanonails. *Nano Letters*, Vol.3, No.2, (February 2003), pp.235-238, ISSN 1530-6984

Li, Q. H.; Wan, Q.; Chen, Y. J.; Wang, T. H.; Jia, H. B. & Yu, D. P. (2004). Stable Field Emission from Tetrapod-like ZnO Nanostructures. *Applied physics Letters*, Vol.85, No.4, (July 2004), pp. 636-638, ISSN 0003-6951

Lu, X. M.; Fanfair, D. D.; Johnston, K. P. & Korgel, B. A. (2005). High Yield Solution-Liquid-Solid synthesis of Germanium Nanowires. *Journal of American Chemical Socierty,* Vol. 127, No.45, (November 2005), pp.15718-15719, ISSN 0002-7863

Nikoobakht, B. & El-Sayed, M. A. (2003). Preparation and Growth Mechanism of Gold Nanorods (NRs) Using Seed-Mediated Growth Method. *Chemistry of Material,* Vol.15, No.10, (April 2003), pp.1957-1962, ISSN 0897-4756

Ohgi, H.; Maeda, T.; Hosono, E.; Fujihara, F. & Imai, H. (2005). Evolution of Nanoscale SnO_2 Grains, Flakes, and Plates into Versatile Particles and Films through Crystal

Growth in Aqueous Solutions. *Crystal Growth & Design*. Vol.5, No.3, (May 2005), pp.1079-1083, ISSN 1528-7483

Pan, Z. W.; Dai, Z. R. & Wang, Z. L. (2001). Nanobelts of Semiconducting Oxides. *Science*, Vol.291, No.5510, (March 2001), pp.1947-1949, ISSN 0036-8075

Pavesi, L.; Dai Negro, L.; Mazzoleni, C.; Franzo, G. & Priolo, F. (). Optical Gain in Silicon Nanocrystal. *Nature*, Vol.408, No.6811, (November 2000), pp. 440-444, ISSN 0028-0836

Patil, D. R.; Patil, L. A. & Patil, P. P. (2007). Cr_2O_3-Activated ZnO Thick Film Resistors for Ammonia Gas Sensing Operable at Room Temperature. *Sensors and Actuators B: Chemical*, Vol.126, No.2, (October 2007), pp.368-374, ISSN 0925-4005

Toury, B.; Bernard, S.; Cornu, D.; Chassagneux, F.; Letoffe, J. M. & Miele, P. (2002). High-Performance Boron Nitride Fibers Obtained from Asymmetric Alkylaminoborazine. *Journal of Materials Chemistry*. Vol.13, No.2, (February 2003), pp274-279, ISSN 0959-9428

Vivekchand, S. R. C.; Gundiah, G.; Govindaraj, A. & Rao, C. N. R. (2004). A New Method for the Preparation of Metal Nanowires by the Nebulized Spray Pyrolysis of Precursors. *Advanced Materials*, Vol.16, No.20, (October 2004), pp.1842-1845, ISSN 1521-4095

Wagner, R. S. & Ellis, W. C. (1964). Vapor-Liquid-Solid Mechnism of Single Crystal Growth. *Applied physics Letters*, Vol.4, No.5, (December 2004), pp. 89-90, ISSN 0003-6951

Wang, Q.; Huang, J.; Xie, Z.; Wang, T. H.; Dattoli, E. N. & Lu, W. (2008). Branched SnO_2 Nanowires on Metallic Manowire Backbones for Ethanol Sensors Application. *Applied physics Letters*, Vol.92, No.10, (September 2008), pp. 102101-102103, ISSN 0003-6951

Wang, X. D.; Song, J. H.; Liu, J. & Wang, Z. L. (2007). Direct-Current nanogenerator Driven by Ultrasonic Waves. *Science*, Vol.316, No.5812, (April 2007), pp.102-105, ISSN 0036-8075

Wang, X. Y.; Zhang, J. Y.; Nazzal, A.; Darragh, M. & Xiao, M. (2002). Electronic structure transformation from a quantum-dot to a quantum-wire system: Photoluminescence decay and polarization of colloidal CdSe quantum rods. *Applied physics Letters*, Vol.81, No.25, (December 2002), pp. 4829-4831, ISSN 0003-6951

Wirtz, M. & Martin, C. R. (2003). Template-Fabricated Gold Nanowires and Nanotubes. *Advanced Materials*, Vol.15, No.5, (March 2003), pp. 455-458, ISSN 1521-4095

Wu, J. M.; Shih, H.C.; Wu, W. T.; Tseng, Y. K. & Chen, I. C. (2005). Thermal evaporation growth and the luminescence property of TiO_2 nanowires. *Journal of Crystal Growth*. Vol.281, No.2, (August 2005), pp. 384-390, ISSN 0022-0248

Yang, P. D. & Lieber, C. M. (1996). Nanorod-Superconductor Composites: A Pathway to High Critical Current Density Materials. *Science*, Vol.273, No.5283, (September 1996), pp.1836-1840, ISSN 0036-8075

Zhang, X. Y.; Zhang, L. D.; Meng, G. W.; Li, G. H.; Jin-Phillipp, N. Y. & Phillipp, F. (2001). Synthesis of Ordered Single Crystal Silicon Nanowire Arrays. *Advanced Materials*. Vol.13, No.16, (August 2001), pp.1238-1241, ISSN 1521-4095

Zheng, B.; Wu, Y. Y.; Yang, P. D. & Liu, J. (2002). Synthesis of Ultra-Long and Highly Oriented Silicon Oxide Nanowires from Liquid Alloys. *Advanced Materials*. Vol.14, No.2, (January 2002), pp.122-124, ISSN 1521-4095

Zhu, Y. C.; Bando, Y.; Xue, D. F. & Golberg, D. (2003). Nanocable-Aligned ZnS Tetrapod Nanocrystals. *Journal of American Chemical Socierty,* Vol. 125, No.52, (September 2003), pp.16196-16197, ISSN 0002-7863

Zott, R. (2003). Friedrich Wilhelm Ostwald (1853–1932), Now 150 Years Young…, *Angewandte Chemie International Edition*, Vol.42, No.34, (September 2003), pp.3990-3995, ISSN 0570-0833

Nanowires - Implementations and Applications

Edited by Dr. Abbass Hashim

ISBN 978-953-307-318-7
Hard cover, 538 pages
Publisher InTech
Published online 18, July, 2011
Published in print edition July, 2011

This potentially unique work offers various approaches on the implementation of nanowires. As it is widely known, nanotechnology presents the control of matter at the nanoscale and nanodimensions within few nanometers, whereas this exclusive phenomenon enables us to determine novel applications. This book presents an overview of recent and current nanowire application and implementation research worldwide. We examine methods of nanowire synthesis, types of materials used, and applications associated with nanowire research. Wide surveys of global activities in nanowire research are presented, as well.

How to reference

In order to correctly reference this scholarly work, feel free to copy and paste the following:

Yajun Tian, Peng Hu and Fangli Yuan (2011). Large-Scale Synthesis of Semiconductor Nanowires by Thermal Plasma, Nanowires - Implementations and Applications, Dr. Abbass Hashim (Ed.), ISBN: 978-953-307-318-7, InTech, Available from: http://www.intechopen.com/books/nanowires-implementations-and-applications/large-scale-synthesis-of-semiconductor-nanowires-by-thermal-plasma

INTECH
open science | open minds

InTech Europe
University Campus STeP Ri
Slavka Krautzeka 83/A
51000 Rijeka, Croatia
Phone: +385 (51) 770 447
Fax: +385 (51) 686 166
www.intechopen.com

InTech China
Unit 405, Office Block, Hotel Equatorial Shanghai
No.65, Yan An Road (West), Shanghai, 200040, China
中国上海市延安西路65号上海国际贵都大饭店办公楼405单元
Phone: +86-21-62489820
Fax: +86-21-62489821

IntechOpen